GEOPHYSICAL RESEARCH LETTERS, VOL. 33, L23706, doi:10.1029/2006GL027831, 2006

Multimodel study of tropical Atlantic variability and change

W.-P. Breugem,[1] W. Hazeleger,[1] and R. J. Haarsma[1]

Received 10 August 2006; revised 30 October 2006; accepted 6 November 2006; published 8 December 2006.

[1] Interannual variability associated with the zonal and the meridional mode in the tropical Atlantic is studied in nine coupled ocean–atmosphere models for twentieth century climate conditions (TC) and the SRES-A1B scenario for future greenhouse gas concentrations. For TC, the subtropical part of the meridional mode is reasonably well simulated, in contrast to the deep tropical part of the meridional mode and the zonal mode. A common model bias is that the onset of the meridional mode is preceded by the presence of a zonal mode in boreal fall that extends towards the western boundary of the Atlantic basin and which initiates a Wind-Evaporation-SST feedback. As a result of this, there is a spuriously strong interaction between the zonal and the meridional mode. The models that seem to best represent the meridional mode show a weakening for future climate conditions. Biases in the zonal mode are too strong to assess changes. **Citation:** Breugem, W.-P., W. Hazeleger, and R. J. Haarsma (2006), Multimodel study of tropical Atlantic variability and change, *Geophys. Res. Lett.*, *33*, L23706, doi:10.1029/2006GL027831.

1. Introduction

[2] Interannual climate variability of the tropical Atlantic is dominated by a meridional and a zonal mode [*Ruiz-Barradas et al.*, 2000; *Xie and Carton*, 2004, and references therein]. The meridional mode is characterized by an SST anomaly confined to the Northern Tropical Atlantic (NTA) and a C-shaped cross–equatorial surface wind anomaly pattern. The zonal mode is characterized by an SST anomaly over the eastern equatorial Atlantic and zonal wind anomalies along the equator. Associated with both modes are shifts in tropical convection that affect rainfall over northeast Brazil [*Moura and Shukla*, 1981] and the African Sahel [*Folland et al.*, 1986] for the meridional mode and the Guinea coast [*Hirst and Hastenrath*, 1983] for the zonal mode. The meridional mode develops in boreal winter and peaks in spring as a result of anomalies in the trade winds and the associated wind-induced latent cooling over the NTA [*Carton et al.*, 1996], along with a positive Wind-Evaporation-SST (WES) feedback [*Chang et al.*, 1997; *Xie*, 1999] acting in the deep western NTA [*Chang et al.*, 2000]. The zonal mode peaks in summer as a result of anomalies in surface zonal winds, SST and thermocline depth, which mutually reinforce each other [*Zebiak*, 1993].

[3] In a previous study changes in the meridional mode for future climate conditions were investigated by means of an atmospheric General Circulation Model (GCM) coupled to a slab mixed layer ocean model [*Breugem et al.*, 2006]. It was found that the WES feedback is phase–locked with the seasonal cycle of the Inter Tropical Convergence Zone (ITCZ), and that changes in the position of the ITCZ may affect the strength and duration of a positive WES feedback and hence the characteristics of the meridional mode. In the present study we investigate the effect of increasing concentrations of atmospheric greenhouse gases on both the meridional and the zonal mode in nine fully coupled ocean–atmosphere GCM's.

2. Models and Simulations

[4] The nine models considered in this study are listed in Table 1. They have been selected from the set of coupled ocean–atmosphere models used for the fourth assessment report of the Intergovernmental Panel on Climate Change (IPCC). Two different sets of simulations have been analyzed. The first set is a simulation of the climate of the twentieth century (20C3M, hereafter TC), covering the period of ~1860 till 2000. The second set is a simulation with the IPCC SRES-A1B emission scenario for a future climate (hereafter FC), starting from 2000 till 2200 (or 2300) and with the atmospheric composition fixed after 2100. In this scenario the atmospheric CO_2 concentration almost doubles over the twenty-first century up to a value of 717 ppmv. For the data analysis monthly means are used. The first 100 years is considered of TC, corresponding to 1861–1960 for the majority of models, and the last 100 years of FC. Linear trends over these periods have been removed from the data.

3. Results

[5] The present paper presents only the main results from this multimodel study; the reader is referred to www.knmi.nl/samenw/tameet/ipcc_ar4_comp for a detailed model comparison. For the analysis of the meridional and the zonal mode we make use of respectively the NTA SST index, defined as the SST anomaly averaged over 55°W–20°W and 5°N–25°N, and the ATL3 SST index, defined as the SST anomaly averaged over 20°W–0°W and 3°S–3°N. These indices have been chosen such that each captures the center of the SST anomaly associated with the respective mode.

3.1. Mean State in TEC

[6] Compared to the ERA-40 reanalysis [*Uppala et al.*, 2005], the averaged SST over the NTA region is generally too low by 1–3°C throughout the seasons. The location of the ITCZ, as computed from the condition of zero meridional wind stress, is offset towards the south in most models [see also *Biasutti et al.*, 2006]. The offset is particularly large for ECHAM5/MPI-OM and CNRM-CM3 in boreal winter and spring, while it is small for UKMO-HadCM3. In all models the SST over the ATL3 region in the eastern

[1]Royal Netherlands Meteorological Institute, De Bilt, Netherlands.

0094-8276/06/2006GL027831$05.00

Table 1. Coupled Ocean-Atmosphere Models Considered in This Study[a]

Model	Run (TC, FC)	Resolution Atmosphere	Resolution Ocean	Reference
CCSM3	6,5	T85L26	1.125° × 0.27° L40	*Collins et al.* [2005]
CNRM-CM3	1,1	T63L45	2° × 0.5° L31	D. Salas-Mélia et al. (Description and validation of the CNRM-CM3 global coupled model, submitted to *Climate Dynamics*, 2006)
CSIRO-Mk3.0	2,1	T63L18	1.875° × 0.84° L31	*Gordon et al.* [2002]
ECHAM5/MPI-OM	1,1	T63L31	1.5° × 1.5° L40	*Jungclaus et al.* [2006]
GFDL-CM2.0	1,1	2.5° × 2° L24	1° × 1/3° L50	*Delworth et al.* [2006]
GFDL-CM2.1	1,1	2.5° × 2° L24	1° × 1/3° L50	*Delworth et al.* [2006]
MIROC3.2(medres)	2,1	T42L20	1.4° × 0.5° L43	*Hasumi and Emori* [2004]
UKMO-HadCM3	2,1	3.75° × 2.5° L19	1.25° × 1.25° L20	*Gordon et al.* [2000]
UKMO-HadGEM1	1,1	1.875° × 1.25° L38	1° × 1/3° L40	*Johns et al.* [2006]

[a]Ocean resolution is given along the equator.

equatorial Atlantic appears too high in JJA, while over the western equatorial Atlantic (west of 30°W) the SST is too low in this season. As a result of this, in most models the equatorial zonal SST gradient in JJA is directed west-east instead of east-west [*Davey et al.*, 2002]. These model biases in the mean state affect the development and structure of the meridional and the zonal mode [*Xie and Carton*, 2004].

3.2. SST Variability in TEC

[7] All models simulate a meridional and a zonal mode in the tropical Atlantic. However, characteristics such as seasonality and amplitude, deviate from observations. Figure 1a shows the variances of the NTA SST and ATL3 SST indices for respectively MAM and JJA (TC). The variance of the MAM NTA SST index is underpredicted by most models. Large differences among the models are found for the variance of the ATL3 SST index. For many models it displays a wrong seasonal cycle, with the maximum value in DJF (CNRM-CM3) or SON (ECHAM5-MPI/OM, CCSM3, UKMO-HadCM3) instead of JJA. Of the models that do have a maximum in JJA, the GFDL models strongly overpredict the variance, while it is strongly underpredicted by MIROC3.2(medres). Because the zonal mode is poorly simulated by all models, we restrict ourselves to analysis of the meridional mode in the rest of this paper.

[8] The structure of the meridional mode in April is depicted in Figure 2 for ERA-40 and for three characteristic models. Compared to ERA-40, the positive SST anomaly over the NTA region extends typically too far towards the equatorial and south Atlantic. A majority of the models shows too strong wind anomalies north of ∼10°N in April, the result of a too long persistence of wintertime trade wind anomalies. The models with a wrong location of the climatological ITCZ, such as CNRM-CM3 and ECHAM5-MPI/OM (Figure 2d), typically underpredict the strength of the C-shaped surface wind pattern in the western equatorial Atlantic.

3.3. Mechanisms of Meridional Mode

[9] To investigate the mechanisms of the meridional mode in TC in more detail, we examine its development in Figure 3. In ERA-40 (Figure 3a), trade wind anomalies emerge north of ∼10°N in January and last till April. As a result of reduction in wind-induced latent cooling, positive SST anomalies start to grow. These SST anomalies trigger a positive WES feedback further to the south. Consequently, SST anomalies also develop in the deep tropics (south of ∼10°N), accompanied by predominantly northward wind anomalies. In boreal summer and fall the anomalies vanish again, because the trade wind anomalies have vanished and the WES feedback has become negative due to migration of the ITCZ towards the north of the deep tropics [*Breugem et al.*, 2006].

[10] In agreement with ERA-40, also in UKMO-HadGEM1 the SST anomalies north of ∼10°N originate from a reduction in wind-induced latent cooling in boreal winter till middle of spring (Figure 3b). This behavior for the subtropical part of the meridional mode is seen for all models, although with differences in strength and persistence of the trade wind anomalies. However, different from ERA-40, UKMO-HadGEM1 shows negative SST anomalies at the equator in both the fall preceding and the fall following the appearance of trade wind anomalies in winter. These negative SST anomalies are likely caused by anom-

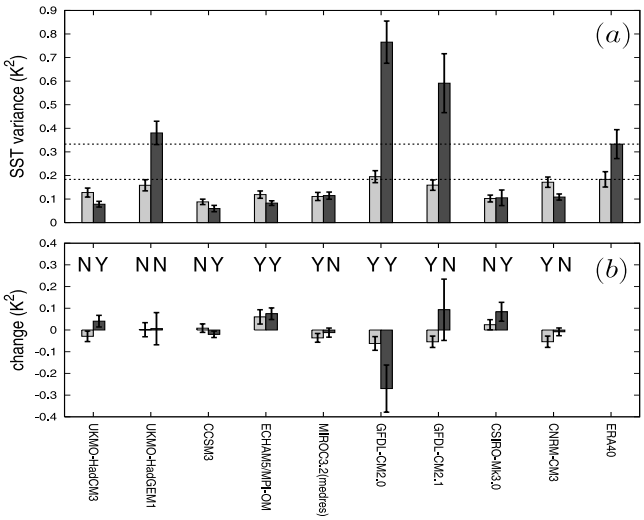

Figure 1. Variances of the NTA SST index for MAM (left bars) and the ATL3 SST index for JJA (right bars). Error bars depict the standard deviation of the variance estimator [*Von Storch and Zwiers*, 2001, p. 84]. (a) TC. Dashed lines represent the values for ERA-40. (b) Difference FC − TC. Letters 'Y' and 'N' indicate whether changes are significant or not, based on a two-tailed F-test at the 10% significance level [*Von Storch and Zwiers*, 2001, p. 119].

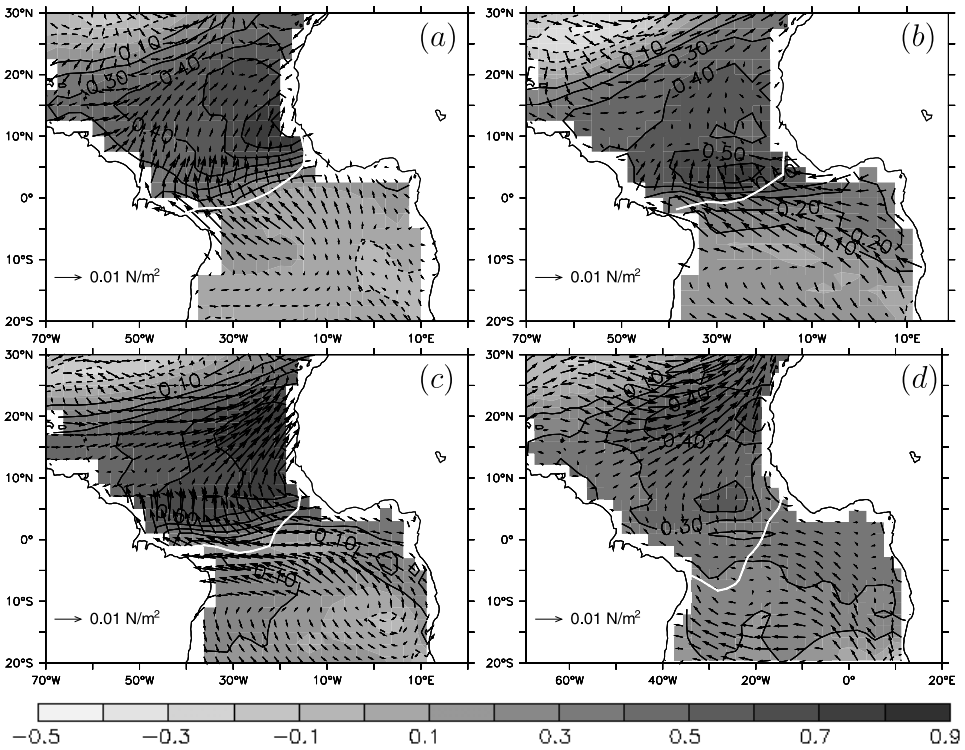

Figure 2. Regressions of anomalous SST (gray colors and black contours, in °C) and wind stress (vectors, in N/m^2) in April onto the MAM NTA SST index, along with the location of the climatological ITCZ (white line). (a) ERA-40. (b) UKMO-HadCM3 (TC). (c) GFDL-CM2.0 (TC). (d) ECHAM5-MPI/OM (TC).

alous upwelling related to anomalous equatorial easterlies and wind stress divergence. They are associated with a zonal mode that extends all the way towards the western boundary of the equatorial Atlantic. We note that the zonal mode is usually thought to be related to anomalies in thermocline depth rather than anomalous upwelling, although this is under debate [*Chang et al.*, 2006]. The equatorial upwelling triggers a positive WES feedback, which maintains or may even reinforce the equatorial upwelling and which causes growth of positive SST anomalies in the deep tropics north of the ITCZ. We will refer to this as the Tropically excited WES (TWES) feedback, to distinguish it from the Subtropically excited WES (SWES) feedback in ERA-40, which is triggered by the appearance of positive SST anomalies north of ~10°N and therefore does not become active earlier than January. The difference between the TWES and the SWES feedback may explain why the largest SST anomaly is located at ~5°N instead of ~15°N for ERA-40.

[11] The interaction between the meridional mode and the fall zonal mode seen for UKMO-HadGEM1 is characteristic for many other models, although usually less strong. Many models show upwelling in the western equatorial Atlantic in fall preceding and/or following the presence of a meridional mode in boreal spring. This triggers a TWES feedback in fall, which causes growth of SST anomalies in the deep tropics (south of ~10°N) independent from the SWES feedback initiated in winter. Furthermore, it is responsible for a decoupling between deep and subtropical SST anomalies and a too weak SWES feedback. This is quantified in Figure 4, which depicts the strength of the interaction between the zonal and the meridional mode against the

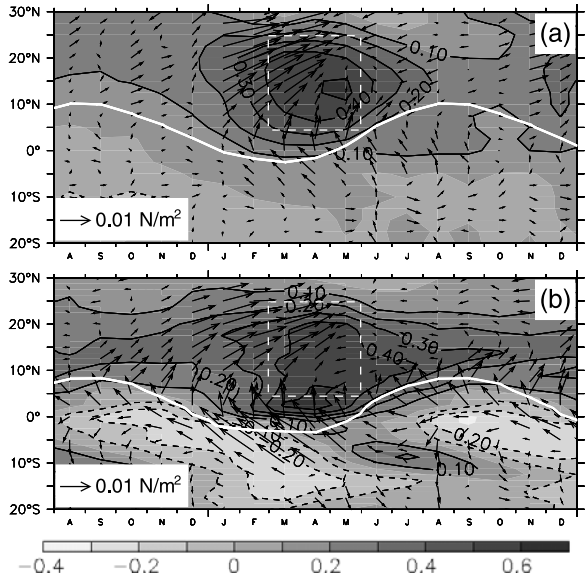

Figure 3. Time-latitude map of lagged regressions of monthly SST (gray colors and black contours, in °C) and wind stress (vectors, in N/m^2) anomalies onto the normalized MAM NTA SST index (dashed rectangle), along with the position of the climatological ITCZ (white line). The anomalies have been zonally averaged over the Atlantic from 55–20°W prior to regression. (a) ERA-40. (b) UKMO-HadGEM1, TC.

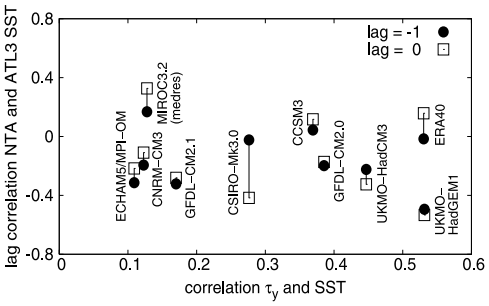

Figure 4. Mode interaction and SWES feedback in TC. Along vertical: lag correlations between MAM NTA SST index and SON ATL3 SST index with SON preceding MAM for lag = −1 and following MAM for lag = 0. Along horizontal: zero lag correlation between meridional wind stress and SST anomalies, which prior to the correlation were averaged over the Atlantic from 55–20°W and respectively 3°S–3°N and 5–15°N.

strength of the SWES feedback. ERA-40 exhibits no mode interaction and a strong SWES feedback, while the majority of the models shows mode interaction and a too weak SWES feedback. Furthermore, ERA-40 has a negligible TWES feedback (−0.1), as computed from the zero lag correlation between SST and meridional wind stress anomalies averaged over 55–20°W and respectively 3°S–3°N and 0–10°N. Contrary to this, all models overpredict the strength of the TWES feedback, notably UKMO-HadGEM1 and CNRM-CM3 (both −0.46). We remark that our finding of no mode interaction in ERA-40 seems to contradict the observational analysis of *Servain et al.* [2000]. However, the southern lob of their dipole SST index for the meridional mode covers the entire equatorial Atlantic between 10°S–5°N, which coincides with the region where the zonal mode manifests itself. This may thus well explain the high correlation value they found between the dipole SST index and their thermocline index for the zonal mode.

3.4. Changes for Future Climate

[12] Relative to TC, in FC the multimodel annual mean SST over the NTA region has increased by 3.1°C to a value of 27.4 ± 1.2°C. Over the same region the magnitude of the annual mean total wind stress decreases in almost all models. The multimodel mean of the total wind stress drops by 4.10^{-3} to a value of $7.5 \cdot 10^{-2} \pm 4 \cdot 10^{-3}$ N/m^2.

[13] Over the ATL3 region the multimodel annual mean SST has increased by 3.2°C to a value of 30.0 ± 0.7°C. Over the same region, the magnitude of the annual mean total wind stress decreases for most models.

[14] The position of the climatological ITCZ changes little for most models. Biggest changes are found for the CSIRO-Mk3.0 and UKMO-HadCM3, which display a northward shift of the ITCZ by a few degrees in boreal winter and spring. Qualitatively similar changes were found in an earlier study [*Breugem et al.*, 2006], where we suggested that this shift causes a weakening of the SWES feedback. The latter is, however, only found for UKMO-HadCM3, not for CSIRO-Mk3.0, possibly because in CSIRO-Mk3.0 ocean heat transport plays a too dominant role in the deep tropical Atlantic.

[15] Changes in the variances of the MAM NTA SST and JJA ATL3 SST indices are shown in Figure 1b for each model. For both indices roughly half of the models shows significant changes, but there is no consistency between the models and changes in the multimodel mean variances appear also negligible. Taking into account that for twentieth century climate conditions UKMO-HadCM3 and GFDL-CM2.0 seem to simulate the meridional mode best of all models (see, e.g., Figures 1a, 2, and 4), we speculate that the meridional mode tends to weaken in future (Figure 1b). Because the zonal mode is poorly simulated by all models, changes in the strength of the zonal mode are difficult to assess.

4. Conclusions

[16] Compared to ERA-40, the models analyzed in this study suffer from a number of biases in simulating the twentieth century tropical Atlantic climate and climate variability. In general, the ITCZ is located too far to the south, the NTA SST is too low all year round, and the ATL3 SST is too high in JJA, the upwelling season for the eastern equatorial Atlantic. It is no surprise that also large model biases are found for the climate variability modes, because the development and structure of these modes depend on the mean state [e.g., *Zebiak*, 1993; *Okajima et al.*, 2003].

[17] The zonal mode is poorly simulated by all models. The majority of the models strongly underpredicts its strength, while the GFDL models strongly overpredict it. For a number of models it peaks in boreal fall or winter instead of summer. Almost all models exhibit also a zonal mode in boreal fall, in agreement with ERA-40, but in this season the SST anomaly pattern extends erroneously towards the western boundary of the Atlantic basin. The presence of SST anomalies in the western equatorial Atlantic initiates a positive TWES feedback, which in some models appears to trigger the development of a meridional mode in the next seasons.

[18] The subtropical part of the meridional mode is reasonably well simulated by the models, and, in agreement with ERA-40, is forced by anomalies in wind-induced latent cooling. The simulation of the deep tropical part of the meridional mode, however, suffers from the interaction with the fall zonal mode and the associated TWES feedback. This decouples the SST anomalies in the deep tropics from the subtropics. The strength of the meridional mode in boreal spring is underpredicted by most models.

[19] No model consistency is found for changes in the strength of the zonal and the meridional mode in future. The two models that seem to simulate the meridional mode best of all models, UKMO-HadCM3 and GFDL-CM2.0, show a weakening of this mode. Further model development is needed to improve the simulation of the equatorial Atlantic before credible statements can be made on changes in the zonal mode.

[20] **Acknowledgments.** We acknowledge the international modeling groups for providing their data for analysis, the Program for Climate Model Diagnosis and Intercomparison (PCMDI) for collecting and archiving the model data, the JSC/CLIVAR Working Group on Coupled Modeling (WGCM) and their Coupled Model Intercomparison Project (CMIP) and Climate Simulation Panel for organizing the model data analysis activity, and the IPCC WG1 TSU for technical support. The IPCC Data Archive at Lawrence Livermore National Laboratory is supported by the Office of

Science, U.S. Department of Energy. This work is funded by the Netherlands Organization for Scientific Research (NWO-ALW, project 854.00.014).

References

Biasutti, M., A. H. Sobel, and Y. Kushnir (2006), AGCM precipitation biases in the tropical Atlantic, *J. Clim.*, *19*, 935–958.

Breugem, W-.P., W. Hazeleger, and R. J. Haarsma (2006), Mechanisms of northern tropical Atlantic variability and response to CO_2 doubling, *J. Clim.*, in press.

Carton, J. A., X. Cao, B. J. Giese, and A. M. da Silva (1996), Decadal and interannual SST variability in the tropical Atlantic Ocean, *J. Phys. Oceanogr.*, *26*, 1165–1175.

Chang, P., L. Ji, and H. Li (1997), A decadal climate variation in the tropical Atlantic Ocean from thermodynamic air–sea interactions, *Nature*, *385*, 516–518.

Chang, P., R. Saravanan, L. Ji, and G. C. Hegerl (2000), The effect of local sea surface temperatures on atmospheric circulation over the tropical Atlantic sector, *J. Clim.*, *13*, 2195–2216.

Chang, P., et al. (2006), Climate fluctuations of tropical coupled systems—The role of ocean dynamics, *J. Clim.*, *19*, 5122–5174.

Collins, W. D., et al. (2005), The Community Climate System Model version 3 (CCSM3), *J. Clim.*, *19*(11), 2122–2143.

Davey, M. K., et al. (2002), STOIC: A study of coupled model climatology and variability in the tropical ocean regions, *Clim. Dyn.*, *18*, 403–420.

Delworth, T. L., et al. (2006), GFDL's CM2 Global Coupled Climate Models. Part I: formulation and simulation characteristics, *J. Clim.*, *19*(5), 643–674.

Folland, C. K., T. N. Palmer, and D. E. Parker (1986), Sahel rainfall and worldwide sea temperatures, *Nature*, *320*, 602–607.

Gordon, C., et al. (2000), The simulation of SST, sea ice extents and ocean heat transports in a version of the Hadley Centre coupled model without flux adjustments, *Clim. Dyn.*, *16*, 147–168.

Gordon, H. B., et al. (2002), The CSIRO Mk3 climate system model, *Tech. Pap. 60*, 130 pp., *CSIRO Mar. and Atmos. Res.*, Hobart, Tasmania, Australia.

Hasumi, H., and S. Emori (Eds.) (2004), K-1 coupled GCM (MIROC) description, *K-1 Tech. Rep. 1*, 34 pp., *Cent. for Clim. Syst. Res.*, Univ. of Tokyo, Tokyo.

Hirst, A., and S. Hastenrath (1983), Atmosphere–ocean mechanisms of climate anomalies in the Angola–tropical Atlantic sector, *J. Phys. Oceanogr.*, *13*, 1146–1157.

Johns, T. C., et al. (2006), The new Hadley Centre Climate Model (HadGEM1): Evaluation of coupled simulations, *J. Clim.*, *19*, 1327–1353.

Jungclaus, J. H., et al. (2006), Ocean circulation and tropical variability in the coupled model ECHAM5/MPI-OM, *J. Clim.*, *19*, 3952–3972.

Moura, A. D., and J. Shukla (1981), On the dynamics of droughts in northeast Brazil: Observations, theory and numerical experiments with a general circulation model, *J. Atmos. Sci.*, *38*, 2653–2675.

Okajima, H., S.-P. Xie, and A. Numaguti (2003), Interhemispheric coherence of tropical Atlantic climate variability: Effect of the climatological ITCZ, *J. Meteorol. Soc. Jpn.*, *81*, 1371–1386.

Ruiz-Barradas, A., J. A. Carton, and S. Nigam (2000), Structure of interannual-to-decadal climate variability in the tropical Atlantic sector, *J. Clim.*, *13*, 3285–3297.

Servain, J., I. Wainer, H. L. Ayina, and H. Roquet (2000), The relationship between the simulated climatic variability modes of the tropical Atlantic, *Int. J. Climatol.*, *20*, 939–953.

Uppala, S. M., et al. (2005), The ERA-40 reanalysis, *Q.J.R. Meteorol. Soc.*, *131*(612), 2961–3012.

Von Storch, H., and F. W. Zwiers (2001), *Statistical Analysis in Climate Research*, 884 pp., Cambridge Univ. Press, New York.

Xie, S.-P. (1999), A dynamic ocean-atmosphere model of the tropical Atlantic decadal variability, *J. Clim.*, *12*, 64–70.

Xie, S.-P., and J. A. Carton (2004), Tropical Atlantic variability: Patterns, mechanisms, and impacts, in *Earth Climate: The Ocean-Atmosphere Interaction*, *Geophys. Monogr. Ser.*, vol. 147, edited by C. Wang, S.-P. Xie, and J. A. Carton, pp. 121–142, AGU, Washington, D. C.

Zebiak, S. E. (1993), Air-sea interaction in the equatorial Atlantic region, *J. Clim.*, *6*, 1567–1586.

W.-P. Breugem, R. J. Haarsma, and W. Hazeleger, KNMI, P.O. Box 201, NL-3730 AE De Bilt, Netherlands. (breugem@knmi.nl)